# Journal of Materials Chemistry A

Accepted Manuscript


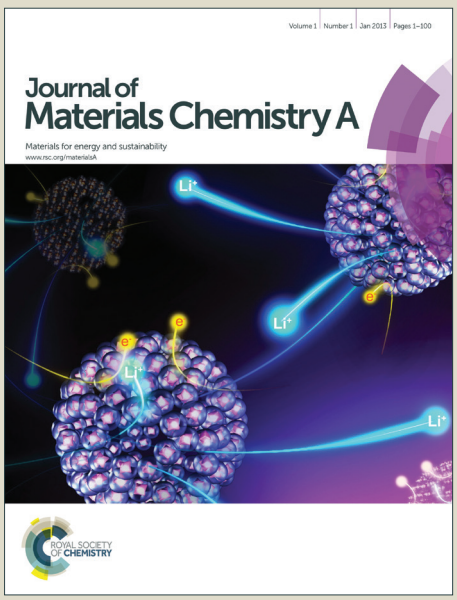





ROYAL SOCIETY OF CHEMISTRY

www.rsc.org/materialsA

Journal of Materials Chemistry A

ARTICLE

# Thermo-stable hollow magnetic microspheres: preparation, characterization and recyclable catalytic applications

Received 00th January 20xx,
Accepted 00th January 20xx

DOI: 10.1039/x0xx00000x

www.rsc.org/

Jingwen Ma,‡[a] Youshen Wu,‡[a] Yun Zeng,[a] Yan Li,[a] Daocheng Wu*[a]

Thermo-stable hollow magnetic microspheres are prepared by layer-by-layer (LbL) assembly on a uniform melamine-formaldehyde resin microsphere template coated by silica and calcination for burning off organic resin. Trypsin is immobilised by their coated polydopamine layer, and nanogolds are assembled onto microspheres by LbL method for catalytic applications. The morphologies and hollow structures are observed by scanning electron microscope and transmission electron microscope. The characteristics are investigated by Fourier transfer infrared spectra, thermo-gravimetric analysis and vibrating sample magnetometer. Meanwhile, the catalytic characteristics of nanogolds and trypsin are evaluated by ultraviolet-visible spectra. The prepared hollow thermo-stable magnetic microspheres are narrow-dispersed with relatively low coefficient of variation, and their size ranging from 0.5 μm to 5.0 μm and saturation magnetization (4-30 emu·g$^{-1}$) can be regulated by different conditions. Combined with magnetic separation and calcination activation or regeneration, these microspheres can also be reused for over 20 times for nanogold catalyst and over 32 times for trypsin catalyst reconjugation without any significant loss in catalytic activity, indicating their considerable potential for recyclable catalytic applications.

## Introduction

Magnetic microsphere is a kind of microsphere that contains magnetic substances and can easily respond under external magnetic field. In the last decades, many researchers have made efforts to fabricate magnetic microspheres and promote their applications. Magnetic microspheres are broadly used in magnetic separation,[1-3] magnetic recoverable immobilised enzyme,[4, 5] magnetic noble metal catalysts,[6, 7] magnetic resonance imaging[8, 9] and other fields.[10, 11]

Magnetic microspheres are also highly valuable substrate for supports used in magnetic recovery with comparatively expensive noble metal catalysts, such as Au, Pt or Pd and associated nanocomponents. Binding of noble metal catalysts to magnetic microspheres allows the retention of these materials at the end of the reaction for reuse,[12-15] preventing the need for additional purification processes to remove the catalyst from the waste stream, thereby making them “greener” catalysts compared with common approaches. Similarly, enzymes can be attached to the surface of magnetic microspheres through chemical conjugation or physical adsorption. Moreover, these microspheres can be used for a range of reactions to produce useful biochemical products, as well as for other applications in biomedical field.[16, 17]

However, in spite of the advantages enabling the retention and removal of the often expensive noble metal and enzymes from the reaction medium, problems associated with the use of magnetic microspheres catalytic systems still exist. The main problem for noble metal catalysts loaded on magnetic microspheres are ineluctable and irreversible catalyst poisoning caused by noble metal catalyst aggregation and organic molecule taking over the active sites, even these catalysts can be used for several times with magnetic separation. Similarly, enzyme can easily lose their activity after catalytic reaction process in case of immobilization enzyme magnetic microspheres. Reconjugation of enzymes to support used in immobilization enzyme magnetic microspheres is very difficult because of the failure in separating the mixture of organic enzymes and inorganic magnetic substances with magnetic separation. Moreover, immobilization enzyme magnetic microspheres are easily precipitated in a solution, hence they have less catalytic reaction time without stirring. Therefore, further innovative approaches are necessary to develop new magnetic noble metal and immobilised enzymatic catalyst systems.

A number of improvements have been reported to overcome the challenges mentioned above. Yao *et al.* reported a magnetic recyclable hollow microsphere Au@polypyrrole (PPy)/$Fe_3O_4$, in which both catalytic nanogolds (AuNPs) and magnetic $Fe_3O_4$ nanoparticles were embedded in the polypyrrole shell polymerizing on 400 nm polystyrene microspheres. The polypyrrole support could stabilise the incorporated nanoparticles and adsorbed substrate. The catalytic activity was still retained even after five cycles, regardless of the loss caused by magnetic recovery.[18] Zhu *et al.* selected magnetic microspheres prepared by hydrothermal method as templates to load catalytic AuNPs. AuNPs that grew *in*

[a] *Key Laboratory of Biomedical Information Engineering of Education Ministry, School of Life Science and Technology, Xi'an Jiaotong University, Xi'an, 710049, P. R. China.*
E-mail: wudaocheng@mail.xjtu.edu.cn; Tel: +86 029 82663941
Electronic Supplementary Information (ESI) available: [details of any supplementary information available should be included here]. See DOI: 10.1039/x0xx00000x
‡These authors contributed equally to this study.

*situ* on the silica-protected magnetic microspheres were still catalytically active even after nine cycles.[19] Nevertheless, they could not be separated from the mixture of organic enzymes and inorganic magnetic substances after several times of recycling catalyst. Only using magnetic separation to solve the problems mentioned above is impossible.

It is noted Wan *et al.* prepared magnetic microspheres by polymerization-induced colloid aggregation method with urea and formaldehyde (UF), in which calcination was utilised to increase the saturation magnetization, while silica was used as an anti-sintering agent to avoid γ-$Fe_2O_3$ from transforming to α-$Fe_2O_3$.[20] This method was improved in our previous study to prepare magnetic microspheres with higher saturation magnetization through UF polymerization induced $Fe_3O_4$ nanoparticle aggregation, in which a silica shell was coated, instead of co-incorporating silica nanoparticles and $Fe_3O_4$ nanoparticles inside the microspheres.[21] High-temperature calcination was then conducted to burn off the UF resin. The results revealed that calcination may be a useful method to separate organic enzymes and inorganic magnetic substances after several times of recycling the catalyst. If thermo-stable magnetic microspheres are used, calcination could not only burn off the organic UF resin and immobilization enzymes, but activates the loaded noble metal in the magnetic microspheres, thereby significantly enhancing the use ration of noble metal catalysts and increasing recyclable times. Different enzymes could also be reconjugated on the thermo-stable magnetic microspheres after calcination, thus, the magnetic microspheres can be reused several times as the immobilization enzyme system.

Based on the aforementioned methods, the novel thermo-stable hollow magnetic microspheres were designed and prepared in this study by layer-by-layer (LbL) assembly on a uniform melamine-formaldehyde (MF) resin microspheres template coated by silica (Scheme 1). First, superparamagnetism iron oxide nanoparticles (SPION) were synthesised using the method reported previously.[22] Uniform MF microspheres were prepared through melamine and formaldehyde polymerization.[23] Second, silica was coated on the surface of the MF microspheres (MF@$SiO_2$) by hydrolysation of tetra-ethoxysilane (TEOS); different layers of negatively charged SPION were fabricated on the surface of MF@$SiO_2$ by polyelectrolyte LbL assembly.[24] Third, thermo-stable hollow magnetic microspheres were obtained by covering another silica layer, followed by calcination at 600 °C in air caused by the burning off MF resin. The saturation magnetization of thermo-stable hollow magnetic microspheres can be adjusted by varying the number of iron oxide nanoparticles layers, and their size was regulated by selecting MF template with different sizes. These microspheres can be easily suspended in aqueous phase because of their hollow structure, which enhances the catalytic time of immobilization enzymes. Combined with magnetic separation and calcination activation or regeneration, these microspheres can also be reused for over 20 times for nanogolds (AuNPs) catalyst and over 32 times for trypsin catalyst without any significant loss in catalytic activity. Their catalyst numbers are much higher than that of magnetic separation reuse. The results of the current study are in agreement with our design. Therefore, thermo-stable hollow magnetic microspheres may have extensive applications in catalytic applications.

## Results and discussion

### Preparation of hydrophilic SPION, silica coated MF microsphere and magnetically adjustable magnetic microsphere

The SPION prepared by thermolysis of organic iron oleate have more attractive advantages than SPION prepared by other methods. The difficulty of its transference to aqueous phase hinders its wide application. To date, several methods are used to transfer hydrophobic SPION to aqueous phase. Liu *et al.* had reported a facile method to transfer hydrophobic SPION to aqueous phase, in which caffeic acid (CA) was introduced as an exchanged ligand to treat oleic acid-capped SPION in hot tetrahydrofuran (THF), meanwhile making SPION negatively charge.[25] MF microspheres were selected as template because of their uniform morphology, narrow dispersion and convenient size control, which was reported

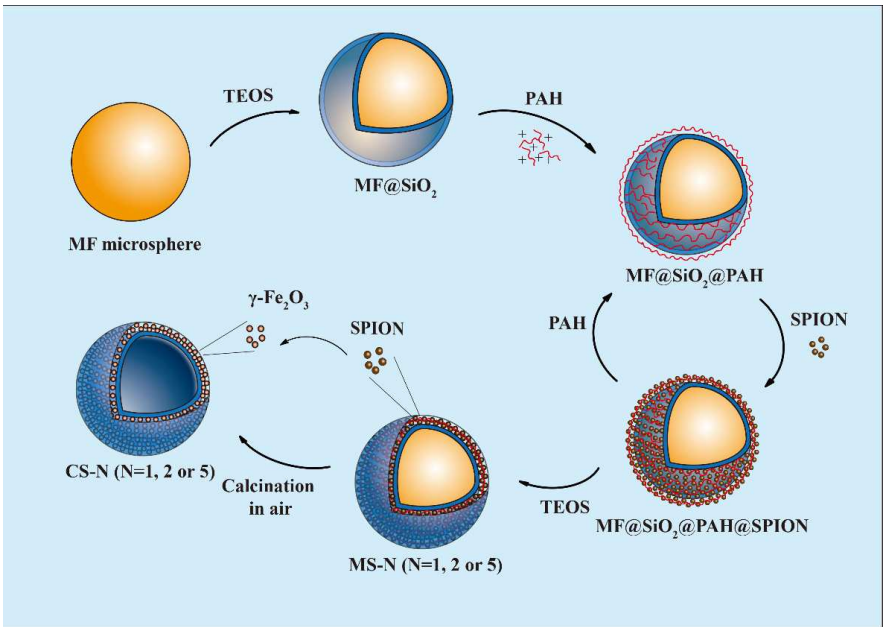


**Scheme 1** Schematic representation the preparation procedures of thermo-stable hollow magnetic microspheres

in our previous research, and importantly, MF organic template could simply be removed by calcination. Recently, MF microspheres with various diameters in the range of 0.5-5.0 μm were synthesised in our research.[23] The size could easily be changed by altering the template size, and the size of MF templates could be changed by varying the reactive condition; at the same time, the size distribution was relatively narrow. Consequently, the magnetic microsphere size could vary from 0.5 μm to 5.0 μm with narrow size distribution, which is deeply dependent on template. In this study, three different sizes (1.5, 1.8 and 2.0 μm) were selected as templates, and related MF microspheres with three different sizes were prepared because size within this range showed better capacity and catalytic activity in both nanogold and trypsin cases, which were associated with the sizes, catalytic load and magnetic content. These MF microspheres covering silica layers with three different sizes were labelled with MF(1.5)@$SiO_2$, MF(1.8)@$SiO_2$ and MF(2.0)@$SiO_2$. Electrostatic interaction promoted the silica coating on MF microsphere. Zeta potential changing from +42 mV to −25 mV indicated the successful silica coating. This silica layer contributed to maintain the original spherical shape of final hollow microspheres after calcination and provided a negative interface for the deposition of the initial poly (allylamine hydrochloride) (PAH) layer.

LbL assembly was a facile method to fabricate magnetically adjustable magnetic microsphere. Although all kinds of three cationic polyelectrolytes [poly (diallyldimethylammonium chloride), polyethyleneimine and PAH] were tested to assemble SPION on MF@$SiO_2$ microspheres, only PAH could successfully incorporate SPION onto silica surface probably caused by the properties of SPION colloid in trishydroxymethylaminomethane (Tris) buffer. Saturation magnetization was readily changed by varying the numbers of SPION-PAH layers. The value of saturation magnetization was closely related with the content of magnetic substance, hence the saturation magnetization could be adjusted by altering the magnetic substance content. LbL assembly was also a facile method of modulating the film thickness precisely, which was used to modulate the magnetic substance content in magnetic microspheres accurately. The other silica layer was covered after ultimate PAH layer attachment in LbL assembly, which could not only prevent the γ-$Fe_2O_3$ transition to α-$Fe_2O_3$,[26] but also guarantee water dispersion after calcination.[27] Microspheres after calcination were labelled as CS-1, CS-2 and CS-5. MF@$SiO_2$ microspheres of three different sizes (1.5, 1.8 and 2.0 μm) were covered with three different numbers of SPION-PAH layers. Thus, a total of nine kinds of magnetic microspheres have been prepared, namely MS(1.5)-1, MS(1.5)-2, MS(1.5)-5, MS(1.8)-1, MS(1.8)-2, MS(1.8)-5 and MS(2.0)-1, MS(2.0)-2 and MS(2.0)-5. After calcination at 600 °C for 3 h in air, these magnetic microsphere were labelled as CS(1.5)-1, CS(1.5)-2, CS(1.5)-5, CS(1.8)-1, CS(1.8)-2, CS(1.8)-5 and CS(2.0)-1, CS(2.0)-2 and CS(2.0)-5. The MS(2.0)-5 without outer silica layer could not disperse in water even after ultrasonic dispersion. Moreover, other opposite charged nanoparticles, such as AuNPs, could be attached on the supports as well, by which a magnetic noble metal catalyst was synthesised in this research.[28] When hollow structure microspheres were obtained, the value of saturation magnetization substantially was raised after removing the organic template by calcination without losing the magnetic property.

**Morphologies**

Figure S1a displayed the transmission electron microscope (TEM) image of SPION morphology. Figure S1b showed the hydrated radius measured by Malvern Zetasizer of both hydrophobic and negative hydrophilic SPION. The average diameter of SPION was 13.0 nm as shown in TEM image, and the diameter of hydrophobic and negative hydrophilic SPION was 12.6 and 16.0 nm, respectively, as measured by Malvern Zetasizer because of the existing hydrated shell on the surface of negative hydrophilic SPION. The zeta potential value of negatively charged hydrophilic SPION was −35 mV in Tris buffer (10 mM, pH 8.5), which was appropriate to assemble with cationic PAH.

Figures S2a and S2b shows the TEM image of citrate-stabilised AuNPs and hydrated radius measured by Malvern Zetasizer, respectively. The average diameter of citrate-stabilised AuNPs was about 10 nm, and its hydrated diameter was 10.1 nm. Meanwhile, Figures S3a, S3b and S3c display the scanning electron microscope (SEM) images of MF(1.5)@$SiO_2$, MF(1.8)@$SiO_2$ and MF(2.0)@$SiO_2$, respectively; MF@$SiO_2$ microspheres were 1.5, 1.8 and 2.0 μm in diameter, respectively. These MF@$SiO_2$ microspheres were mono- or narrow-dispersed with relatively low coefficient of variation (CV) [MF (1.5)@$SiO_2$ (CV<3%), MF (1.8)@$SiO_2$ (CV<3%), MF (2.0)@$SiO_2$ (CV<4%)], which were determined by measuring at least 200 microspheres.

Figure 1 showed the SEM images before and after calcination of MS(2.0)-1, MS(2.0)-2, MS(2.0)-5, CS(2.0)-1, CS(2.0)-2 and CS(2.0)-5; the average diameters of MS(2.0)-1, MS(2.0)-2 and MS(2.0)-5 were 2.1 μm, and the diameters of CS(2.0)-1, CS(2.0)-2 and CS(2.0)-5 were slightly smaller. The diameters slightly increased with the increasing SPION layers because of the attachment of PAH-SPION layers and outer silica coating. Similarly, MS(1.5)-1, MS(1.5)-2, MS(1.5)-5, CS(1.5)-1, CS(1.5)-2 and CS(1.5)-5 were shown in Figs. S4a1, S4b1, S4c1, S4a2, S4b2 and S4c2.

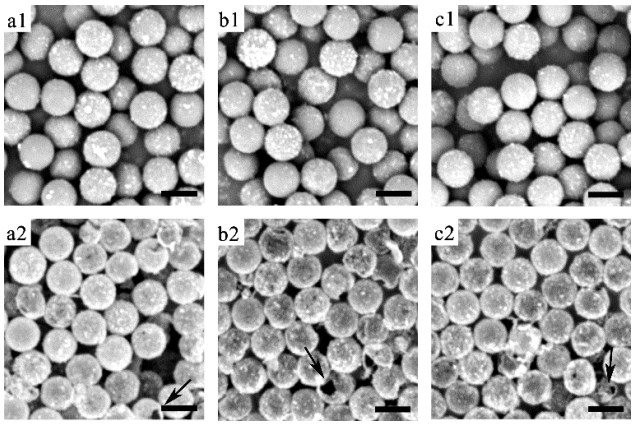


**Fig.1** SEM images of MS(2.0)-1 (a1) , MS(2.0)-2 (b1) and MS(2.0)-5 (c1) and CS(2.0)-1 (a2), CS(2.0)-2 (b2) and CS(2.0)-5 (c2). Scale bar in each image = 2 μm.

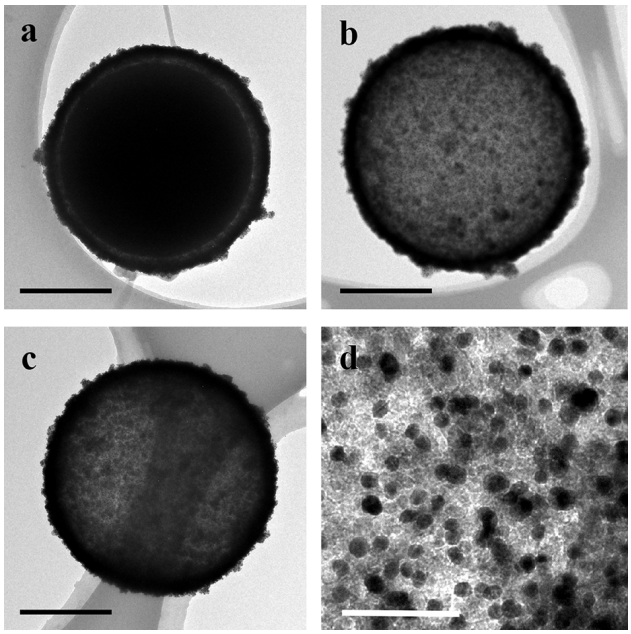


**Fig.2** TEM images of MS(2.0)-5 (a), CS(2.0)-5 (b), CS(2.0)-5 after calcination for five times (c). Feature of partial CS(2.0)-5. Scale bar in (a), (b) and (c) = 1 μm and (d) = 100 nm.

The average diameter of MS(1.5)-1, MS(1.5)-2, MS(1.5)-5, CS(1.5)-1, CS(1.5)-2 and CS(1.5)-5 were about 1.6 μm. Part of the shades implied the hollow structure after calcination. In parallel, MS(1.8)-1, MS(1.8)-2, MS(1.8)-5, CS(1.8)-1, CS(1.8)-2 and CS(1.8)-5 were respectively shown in Figs. S5a1, S5b1, S5 c1, S5a2, S5b2 and S5c2. The average diameter was 1.9 μm, as shown in SEM images. Less broken microspheres in MS(1.5) cases were observed after calcination because less gas was produced during MF template decomposition.

Actually, seldom of microspheres could suffer from burst in the calcination process because MF microspheres were chosen as template. MF microspheres performed better thermal stability when compared with polystyrene microspheres or urea-formaldehyde resin microspheres, which was benefit that carbonization and gradual pyrolysis, rather than vaporization takes place during calcination.[23] This phenomenon could be seen in Fig. S6. The SEM images of CS(1.5)-5, CS(1.8)-5 and CS(2.0)-5 were shown in Fig. S6a, S6b and S6c, respectively. Only a few broken microspheres could be found in these three kind of microspheres.

Figures 2a and 2b displayed the TEM images of solid MS (2.0)-5 and the hollow structure of CS(2.0)-5 after calcination for the first time, respectively. And after calcination for the fifth time, TEM image of CS(2.0)-5 are shown in Fig. 2c. In Figs. 2b and 2c, the γ-$Fe_2O_3$ nanoparticles are clearly seen and bigger nanoparticles that were the silica nanoparticles produced in Stöber method. The details of Fig. 2c was shown in Fig. 2d. The outer amorphous and porous $SiO_2$ matrix acting as an anti-sintering agent could prevent γ-$Fe_2O_3$ from transforming to α-$Fe_2O_3$ by spatially restricting the growth of nanoparticle size, which could remarkably increase the phase transition temperature. After calcination, the size of γ-$Fe_2O_3$ nanoparticles maintained the initial size (13 nm), and rather larger α-$Fe_2O_3$ reported 35 nm in Fig. 2d. This phenomenon was also reported in our previous research.[21] From SEM and TEM images, a slight change in diameter was observed after calcination. Most of the microspheres were entirely apart from a few shards observed in microspheres after calcination and part of microspheres with holes, which were pointed out by arrow in Fig. 1 and suggested that the hollow structure was obtained after calcination. Silica coating could not only maintain the hollow spherical structure after calcination, but also prevent phase transformation at high temperature. Additionally, TEM images of SPION before and after assembly were also shown in Fig. S7a and S7b, respectively. Size of SPION before and after assembly was about 13 nm. Size distribution did not change after assembly and aggregation did not take place either.

**Fourier-transform infrared (FTIR) spectra, X-ray diffractometer (XRD) spectra, vibrating sample magnetometer (VSM), zeta-potential variation and magnetization curves**

Figure 3a showed the FTIR spectra of SPION (a1), MS (2.0)-5 (a2) and CS(2.0)-5 (a3). Peaks at 631 and 584 $cm^{-1}$ represent the Fe-O characteristic peaks. The N-H and O-H stretching vibrations appeared at 3156 and 3398 $cm^{-1}$. Meanwhile, the C=O and C–N stretching vibrations appeared at 1559 and 1343 $cm^{-1}$. The peaks at 1092 $cm^{-1}$ correspond to the asymmetric stretching vibration of Si-O-Si. In the FTIR spectra of CS(2.0)-5 (a3), only Fe-O characteristic peaks and Si-O-Si asymmetric stretching vibration peaks were left, indicating that most organic template and polyelectrolyte were removed after calcination.[29, 30] Figure 3b shows the XRD spectrum of both MS(2.0)-5 and CS(2.0)-5. Before calcination, the diffraction peaks [(220), (331), (222), (400), (422), (511), (440), (533)] match with $Fe_3O_4$ (JCPDS no. 65-3107), which was shown as line b1.[31]The diffraction peaks [(220), (311), (400), (422), (511), (440) and (533)] matched with γ-$Fe_2O_3$ (JCPDS no. 39-1346) shown as line b2, which was confirmed in our previous research.[21] Furthermore, the wide diffraction peaks at 2θ=22° (JCPDS No. 29-0085) consisted of amorphous silica.[32] The sandwich-like structure of CS(2.0)-5 could retain its magnetism because the existence of $SiO_2$ prevented γ-$Fe_2O_3$ from transforming to α-$Fe_2O_3$ during calcination in the air.

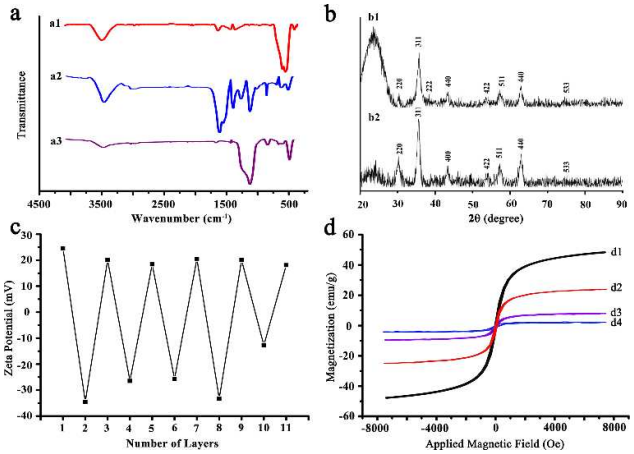


**Fig.3** FTIR spectra of SPION (a1), MS(2.0)-5 (a2), CS(2.0)-5 (a3). XRD pattern of MS(2.0)-5 (line b1) and CS(2.0)-5 (line b2). The alternative Zeta-potential value in Tris (10 mmol·$L^{-1}$, pH 8.5) buffer. Magnetic hystersis loop of SPION (d1), CS(2.0)-5 (d2), CS(2.0)-2 (d3) and CS(2.0)-1 (d4).

Furthermore, $SiO_2$ layers contributed to maintain the shape and water dispersion after calcination, which had been explained earlier. The change in zeta potentials of the samples measured in Tris (10 mmol·$L^{-1}$, pH 8.5) buffer were represented in Fig. 3c. When PAH and SPION were attached onto MF@$SiO_2$ surface, the zeta potential value reached about +23 mV and −30 mV, respectively. The alternative zeta potential value demonstrated the electrostatic adsorption between positive PAH and negative SPION. The final PAH layer gained access to the outer silica layer coating.[33]

The magnetic properties of magnetic microsphere with different SPION layers were tested, and the hysteresis loops of SPION (d1), CS(2.0)-5 (d2), CS(2.0)-2 (d3) and CS(2.0)-1 (d4) were shown in Fig. 3d. The saturation magnetization of SPION was 48.27 emu·$g^{-1}$. The saturation magnetization values of magnetic microspheres after calcination increased with the increasing number of SPION layers, which was clearly shown in Fig. 3d. Meanwhile, the saturation magnetization of CS(2.0)-5 (d2), CS(2.0)-2 (d3) and CS(2.0)-1 (d4) was 25.41, 10.99 and 3.37 emu·$g^{-1}$, respectively. The difference of saturation magnetization was caused by the different γ-$Fe_2O_3$ nanoparticle contents. The more γ-$Fe_2O_3$ nanoparticles resulted in the higher value of saturation magnetization. The amount of SPION in CS(2.0)-5 was 19.09%, which was determined by inductively coupled plasma-atomic emission spectrometry (ICP-AES). No significant difference was observed in size, although the saturation magnetization was substantially increased from 3.37 emu·$g^{-1}$ for CS(2.0)-1 and 10.99 emu·$g^{-1}$ for CS(2.0)-2 to 25.41 emu·$g^{-1}$ for CS(2.0)-5 because the thickness of cationic polyelectrolyte and SPION layers was too thin to change the whole sphere diameter significantly. This method of adjusting magnetism by LbL assembly was also suitable for MS(1.5)@$SiO_2$ and MS(1.8)@$SiO_2$ as well. Figure S8b shows that the values of saturation magnetization were 4.85, 10.29 and 32.19 emu·$g^{-1}$ for CS(1.5)-1, CS(1.5)-2 and CS(1.5)-5, respectively. Meanwhile, the saturation magnetization values were 5.25, 14.16 and 27.98 emu·$g^{-1}$ for CS(1.8)-1, CS(1.8)-2 and CS(1.8)-5, respectively, as shown in Fig. S8c. Furthermore, the saturation magnetization largely increased from 4.47 emu·$g^{-1}$ [MS(2.0)-5] to 25.41 emu·$g^{-1}$ [CS(2.0)-5] after MF template calcination for the first time because of the increased in the magnetic substance content, and the value achieved 27.98 emu·$g^{-1}$ during the second calcination because of the residual organic part clearance, which was shown in Fig. S8a. Therefore, calcination to remove the organic template was an effective approach to increase the saturation magnetization value.

**Thermo-gravimetric analysis (TGA) and different scanning calorimetry (DSC) and separation**

Figure 4a showed the TGA results of both MS (2.0)-5 with and without the outer silica layer. The weight loss under 400 °C was attributed to water evaporation and low molecular weight organic molecule thermolysis. The weight abruptly decreased at 400 °C as MF resin polymer started pyrolysis. As temperature increased from 400 °C to 800 °C, the weight of microspheres was gradually lost. The final weight percentage of MS(2.0)-5 with outer silica layer was slightly higher than MS(2.0)-5 without outer silica layer, resulting from more silica component in the former.

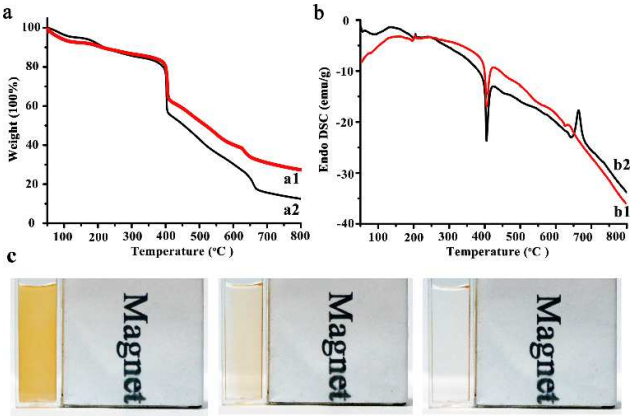


**Fig.4** TGA curve of MS(2.0)-5 (a1) and MS(2.0)-5 without outer silica layer (a2). DSC curve of MS(2.0)-5 (b1) and MS(2.0)-5 without outer silica layer (b2). Separation of CS(2.0)-5 under external magnetic field (c).

The DSC results in Fig. 4b showed that an extra corresponding exothermic peak at 600 °C appeared in MS(2.0)-5 without the outer silica layer (Fig. 4b1); on the contrary, no peak was observed in MS (2.0)-5 with the outer silica layer shown in Fig. 4b2, which indicated that the outer silica layer played an important role in maintaining the crystal structure of γ-$Fe_2O_3$ and agreed with the TEM image in Fig. 2d and the XRD spectra results.[21] Figure 4c presents the separation states. The hollow magnetic microspheres could be rapidly recovered under external magnetic field within 90 s, benefiting from its high saturation magnetization, which largely simplified the operational procedures and saved the equipment cost.

**Energy Dispersive X-ray Detector (EDX) mapping and sedimentation state**

Characterizations of AuNPs loading magnetic recyclable catalytic microspheres are shown in Fig. 5a and 5b. The TEM image of EDX spectra and EDX mapping of CS(2.0)-5-Au after calcination for the first time are shown in Figs. 5a1, 5a2 and 5a3, respectively. The TEM image of Energy Dispersive X-ray Detector (EDX) spectra and EDX mapping of CS(2.0)-5-Au after calcination for the fifth time were shown in Figs. 5b1, 5b2 and 5b3, respectively. The element distribution of Fe, Au, Si and O of CS(2.0)-5-Au after calcination for the first time and for the fifth time were analysed. There were no differences in Au nanoparticles content and distribution after calcination for many times, indicating there were no affects in AuNPs distribution under calcination in the presence of silica as an anti-sintering agent. The hollow structure was obtained after calcination, which ensured the long suspension time of these magnetic microspheres. Unlike magnetic nanoparticles stabilised by colloidal properties, the magnetic microspheres could not suspend well in aqueous phase. The sedimentation time of magnetic microspheres in aqueous phase had not been emphasised in previous research because most of the magnetic microspheres were solid microspheres. The long suspension time of magnetic microspheres benefited the magnetic separation, magnetic recovery and other magnetic microsphere applied fields. Sedimentation state of both MS(2.0)-5 and CS(2.0)-5 was recorded

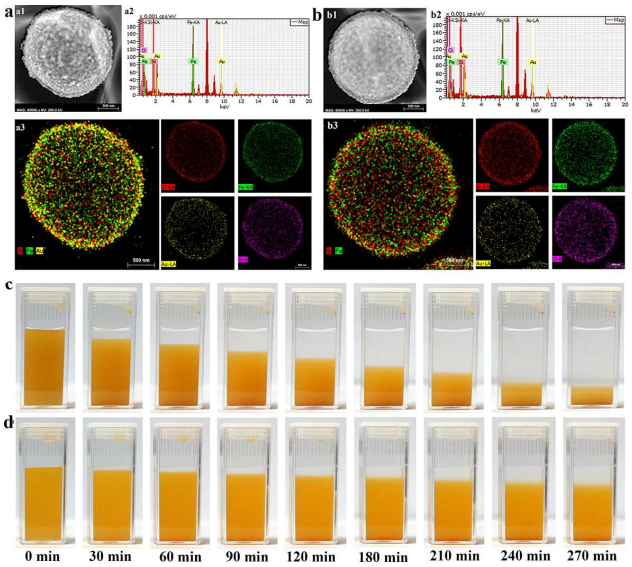


**Fig.5** CS(2.0)-5-Au after calcination for the first time in (a): TEM images (a1), EDX spectra (a2) and EDX mapping (a3); CS(2.0)-5-Au after calcination for the fifth time in (b): TEM images (b1), EDX spectra (b2) and EDX mapping (b3); The sedimentation statement of MS(2.0)-5 (c) and CS(2.0)-5 (d) at different time point.

at 0, 30, 60, 90, 120, 150, 180, 210, 240 and 270 min in Figs. 5c and 5d. MS(2.0)-5 sank quicker than CS(2.0)-5. The difference appeared at 30 min and until 270 min. MS (2.0)-5 mostly sank to the bottom, but CS(2.0)-5 was partially suspended in aqueous phase. The magnetic microspheres with hollow structure showed about three times better than solid ones. Although many kinds of magnetic hollow microspheres or capsules were reported, the low-saturation magnetization, irregular size distribution and the thermo-instable organic matrix made them unsuitable in magnetic recovery and catalyst regeneration based on magnetic materials. The hollow structure probably had more advantages compared with solid microspheres besides the enhancement in saturation magnetization. Microspheres with hollow structure would suspend for longer time than solid structure, without the losing saturation magnetization. The magnetic substance with high density spread in shell rather than in core and the 5 layers of $SiO_2$/SPION/$SiO_2$ sandwich structure should be more resistant than the thin silica shell against high temperature, thereby resulting in seldom collapse during calcination. These magnetic microspheres with hardened shell not only possessed strong mechanical strength, but also high content of magnetic substance, which overcame the present magnetic microspheres that were neither low-density with low-saturation magnetization nor high density with high-saturation magnetization. These high-saturation magnetization and low-density magnetic microspheres with hollow structure gave a possibility to react adequately without string and separate rapidly. Therefore, the magnetic microspheres with hollow structure were more suitable for catalyst application and separation in aqueous phase as a support.

**Magnetic recovery and regeneration of immobilised trypsin**

Many crosslinking methods, including both physical and chemical methods, have been utilised to immobilise protein on the surface of microspheres. Polydopamine has been proven to be a faultless method, has been utilised to immobilise protein on the surface of microspheres. Schiff base interaction took place between amino groups or thiol groups of protein and catechol/quinone existing on polydopamine layer because the catechol could be oxidised to quinone in alkaline solution.[34] Dopamine (DA) polymerises on various solid supports by directly soaking in Tris (10 mmol·$L^{-1}$) buffer. In our experiment, polydopamine was deposited on microspheres [CS(2.0)-5@PDA] with hollow structure for further protein immobilization. After polydopamine coating, CS(2.0)-5@PDA appeared darker than CS(2.0)-5 because of the black polydopamine.[35] Bovine serum albumin (BSA), as a model protein, was immobilised on CS(2.0)-5@PDA in this experiment. Finally, about 63 μg of BSA was immobilised onto CS(2.0)-5@PDA per milligram. Meanwhile, trypsin was 29.7 μg·$mg^{-1}$ [CS(2.0)-5@PDA], probably due to the difference in protein properties, for instance different properties of isoelectric point and number of amino groups per protein molecule. Both quantities of the immobilised protein were identified by Bradford method.

N-benzoyl-L-arginine ethyl ether (BAEE) was introduced as substrate to test trypsin activity before and after immobilization. Table 1 showed the values of relative activity in each cycle. The natural trypsin activity was 3500 Unit·$mg^{-1}$, and after immobilization, its activity turned to about 80% compared with the activity of natural structure probably caused by the lesser contact area between substrates and enzyme and some changes in trypsin conformation.[36] After eight times of recycling, the magnetic microspheres that immobilised trypsin became inactive and were calcined in the air to burn off the organic compound for trypsin re-immobilization in Scheme 2, and the regeneration was carried out for three times. The values of relative activity after re-immobilization in each recoverable cycle were recorded in Table 1. No difference in trypsin activity was observed among these re-immobilization procedures, therefore indicating that this method was a practical way to regenerate immobilised enzyme based on thermo-stable magnetic microspheres. Lin *et al.* immobilised trypsin on magnetic microspheres covered with 3-glycidoxypropyl-trimethoxysilane (GLYMO) to detect the properties in microwave-assisted protein digestion application. The trypsin activity was reported only for eight reproducing times, and the sequence

**Table 1** The relative activity of immobilized Trypsin for magnetic recovery in each regeneration

| | Calcination 1 | Calcination 2 | Calcination 3 | Calcination 4 |
|---|---|---|---|---|
| Cycle 1(%) | 83.33 | 88.34 | 82.47 | 89.34 |
| Cycle 2(%) | 85.03 | 76.35 | 84.09 | 83.07 |
| Cycle 3(%) | 71.67 | 83.32 | 81.95 | 91.20 |
| Cycle 4(%) | 75.05 | 90.06 | 90.41 | 90.37 |
| Cycle 5(%) | 78.33 | 81.39 | 89.38 | 90.10 |
| Cycle 6(%) | 91.33 | 75.13 | 91.68 | 89.62 |
| Cycle 7(%) | 88.35 | 85.24 | 88.91 | 89.03 |
| Cycle 8(%) | 80.38 | 76.51 | 90.73 | 88.74 |

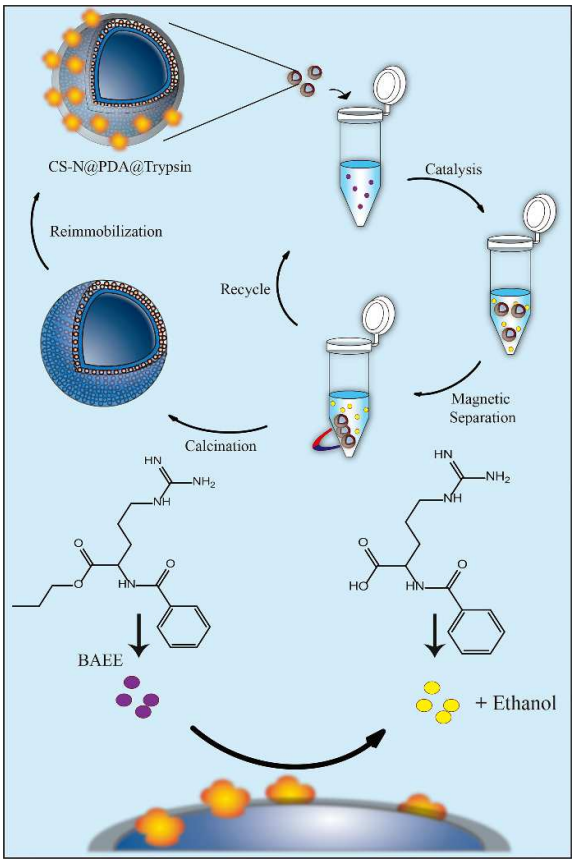


**Scheme 2** Immobilization of Trypsin on CS(2.0)-5, the magnetic recycle as well as regeneration by calcination

coverage was about 80% in each cycle.[37] A total of 11 recyclable times were available for trypsin immobilised on magnetic nanoparticles applied for proteolysis in that of Li *et al.* report, which showed that the sequence coverage of Trypsin was about 70%, and trypsin activation of Trypsin decreased since the ninth cycle.[38] In that of Lin *et al.* research, eight recyclable times were available for trypsin immobilised on magnetic beads covered with GLYMO, and sequence coverage was only about 20%.[39] The reusable times in the previous researches were relatively poor. The recyclable times of our microspheres with immobilization trypsin could be remarkably enlarged to 32 times, which immensely ameliorated the properties of immobilised trypsin.

Furthermore, the regeneration of immobilised enzyme was a challenge for its application because separating the chemical crosslinking enzyme from the supports is difficult. From now on, in order to realize immobilized enzyme regeneration, some approaches had been put forward, such as metal ion chelation, DNA single strands complementation, direct crosslink on inactive enzyme by glutaraldehyde.[40-42] There were still some limits in application. For example enzyme which could not chelate with metal ion was not suitable in metal ion chelation case, DNA complementation would be broken in high temperature situation and magnetic properties could be critically influenced when excessive inactive enzyme immobilized on supports. In our previous research, calcination was found to be an effective method to remove organic compound from inorganic compound, which was hopeful to be utilized in immobilized enzyme regeneration.[21] As a result, thermal-stable hollow structure magnetic microspheres were fabricated by LbL assembly and silica as an anti-sintering agent was introduced to maintain magnetic properties. In current study, enzymes can be mildly immobilized to the thermo-stable hollow magnetic microspheres and maintained over 85% of average enzymes activation after 32 times of cycle use (Table 1). These results are evidently superior to those magnetic carriers discussed above. Polydopamine was involved in to immobilized trypsin and both of enzymes and polydopamine could be removed by calcination. Then this process could be operated for another time to regenerate enzymes without influences in activation. Although the crosslinking degree and surface properties of silica surface changed during calcination, dopamine could deposit on various surfaces in Tris buffer, regardless the change in silica surface. The polydopamine cross-linker could overcome the disadvantages of functionalization by silica-coupling agent on high-temperature-treated silica. The operation was much easier than methods discussed above. In addition, other enzymes apart from trypsin might be immobilized to the microspheres as well. Thus, this was a facial, practicable and universal method to realize immobilized enzyme regeneration. Meanwhile, the activation of enzymes was maintained higher than that of reported previously.

**Catalytic reduction of methylene blue (MB) dye and the reactivation of heterogeneous catalyst**

As a high-performing noble metal catalyst, AuNPs were proven for application in carbon-carbon coupling reaction, hydrogenation and various dye reductions.[43-45] MB was selected as a model pollutant to test the catalyst activity of CS(2.0)-5-Au in waste water treatment on the condition that sodium borohydride ($NaBH_4$) introduced as reducing agent.[46] In this case, AuNPs were immobilised on MS(2.0)-5 by LbL assembly and reactivated by calcination, as shown in Fig. 6a, by which could accurately control the quantity of incorporated AuNPs identified by ultraviolet-visible (UV-vis) absorption [1.38 mg per 10 mg of MS(2.0)-5 without outer silica layer]. Figure S9 illustrated the changes in the absorption spectrum of MB solution during the reduction at different time points (0, 1, 2 and 3 min). The maximum absorption peak of MB molecule disappeared in 3 min, thus indicating that the action was completely finished. The reaction should be regarded as pseudo-first-order reaction for the superfluous $NaBH_4$ placed into the reactive system. The reaction rate constant of each cycle was calculated by the slope of $\ln(C_t/C_0)$, in which $C_t$ represents the MB solution concentration at t, and $C_0$ represents the MB solution concentration at 0. For the first calcination, the respective rate constant values were 0.5453, 0.2387, 0.2126, 0.2085 and 0.1644 $min^{-1}$, as shown in Fig. 6b. The rate constant value gradually decreased because of the catalyst damage. This phenomenon was reported in many researches because some organic molecules combined the active site on the surface of AuNPs, which was difficult and universal problem in catalyst recovery. The magnetic recovery cycle experiments were also carried out for five times after reactivation by calcination, and the rate constants were 0.4616, 0.3843, 0.2308, 0.1317 and 0.0781 $min^{-1}$ after second calcination time. In the third calcination time, the values were 0.5208, 0.4026, 0.2114, 0.1446 and 0.1175 $min^{-1}$

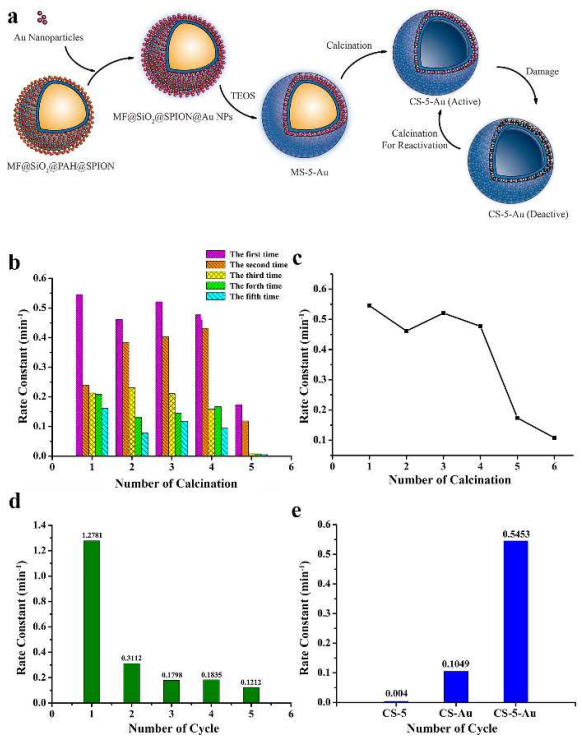


**Fig.6** Scheme for CS(2.0)-5-Au fabrication and reactivation (a).The catalytic rate constant of CS(2.0)-5-Au for each magnetic recycle in every calcination reactivation (b). The rate constant tendency of CS(2.0)-5-Au for the first catalytic reaction in every calcination reactivation (c). The catalytic rate constant of MS(2.0)-5-Au in magnetic recovery for five times in (d) The catalytic rate constant of CS(2.0)-5, CS(2.0)-Au and CS(2.0)-5-Au (e).

(data shown in Fig. 6b). During the fourth calcination, the rate constant values were 0.4773, 0.4314, 0.1587, 0.1670 and 0.0941 $min^{-1}$ (data shown in Fig. 6b). In the fifth recycle, the rate constant values were 0.1737, 0.1185, 0.0078, 0.0074 and 0.0052 $min^{-1}$ (data shown in Fig. 6b). The sixth recycle was also carried out, and thecatalytic rate constant value was 0.1082 $min^{-1}$ for the first time, and the value was as low as 0.0155 $min^{-1}$ for the second time, hence indicating the catalytic activity was lost (data not shown). From the above results, in each repetition of calcination, the rate constant values for each magnetic recycle were lower, which explained that the catalyst was damaged. Once calcination was conducted, the catalytic activity was mostly recovered from the former four times of calcination, and this damaging process occurred again. Unfortunately, only partial activity could be recovered in the fifth calcination, and the catalytic rate constant value was much lower in the sixth calcination. Figure 6c showed the variation tendency of the rate constant values in the first catalytic reaction in each calcination repetition. The values in the former four times were similar, but after four calcination, the rate constant value became lower. The rate constant value gradually decreased, which was attributed to the following two reasons: ineluctable loss in recovery process and aging of catalyst. The previous magnetic recovery AuNPs catalyst had shown five or a little more reuse times in recycle assay and seldom could achieve more than 10 reuse times, probably due to the deactivation or aggregation of AuNPs. The $SiO_2$@$Fe_3O_4$/C@Au magnetic catalyst reported by Zeng *et al.* could be reused for nine times without further reuse in nitrophenol reduction.[47] Meanwhile, only six repetition of $Fe_3O_4$@C@Ag–Au composite microspheres in nitroaromatic compound reduction was reported in that of An *et al* report.[48] AuNPs immobilised on $Fe_2O_3$-graphene oxide nanosheets were prepared in Woo *et al.* report, and the recyclable procedures were carried out for merely seven times.[49] To further resolve this problem, the calcination process was introduced in our research to clear up the repugnant organic small molecule. The active site of AuNPs in the CS(2.0)-Au would be reused after calcination by removing the occupying organic small molecule. Silica acting as an anti-sintering agent could avoid aggregation of both AuNPs and SPION during calcination, and the fixation to Au NPs could ensure the diffused state without losing catalytic activation.[49] Our thermo-stable hollow magnetic microspheres with AuNPs catalyst could be recycled for over 20 times of use, as shown in Fig. 6b, which was significantly higher than the previous number of research. The restored catalytic activity after calcination indicated that calcination should be a feasible way of reactivating the aging catalyst. The rate constant values of MS(2.0)-5-Au and recovery experiment were also recorded, which were 1.2787, 0.3112, 0.1798, 0.1835 and 0.1212 $min^{-1}$, as shown in Fig. 6d. The aging situation as also presented in the MS(2.0)-5-Au case. The reactive rate constant of MS(2.0)-5-Au was higher than CS(2.0)-5-Au for the first time, which was probably due to the microstructure change of amorphous silica and the high-temperature-induced compact combination between silica and AuNPs. Silica had been used as an anti-sintering agent in a number of research to restrict AuNPs sintering during calcination, which was similar in the SPION case treatment. The inserted figure in Fig. S9 was taken after five cycles. A considerable number of research pointed out that the nano-interface between noble metal and metal oxide can enhance the catalytic ability because of stronger electronic interaction. In Fig. 6e, the rate constant of CS (2.0)-5, CS(2.0)-Au and CS(2.0)-5-Au were compared totally, and the values were 0.004, 0.1049 and 0.5453 $min^{-1}$, respectively. In addition, the rate constant of microspheres with both AuNPs and SPION (0.5453 $min^{-1}$) were about five times higher than microspheres with only AuNPs (0.1049 $min^{-1}$), which might owe to formation of heterogeneous nanointerface between part of AuNPs and SPION in calcination providing an easy way to create heterogeneous nanointerface. CS(2.0)-5-Au contributed as a brilliant catalyst in reducing MB molecule and could be reactivated by calcination, thus resolving the catalyst aging challenge.[51, 52] In our study, similar to regeneration of immobilized trypsin, we also used calcination to activate attached noble metal catalyst, the results were encourage and 20 recycled times of catalyst could be obtained that was significant higher than that of previously recyclable noble metal catalysts. The feature of our noble metal activation strategy was combination of magnetic separation and calcination activation. That was the innovation for the improvement of the recyclable noble metal catalyst. In contrast, the previous magnetic recyclable noble metal catalysts were only associated with magnetic separation. Therefore, calcination could either prepare recyclable thermo-stable hollow magnetic microspheres or activated attached noble metal catalyst, thus prolong their recycled times for catalysis. In addition, abandoned magnetic microspheres will pollute

environments. In case of magnetic noble metal catalyst, noble metal materials are expensive and difficultly degradable. Increase recycled times means the lower costs and less pollutes.

## Experimental

### Materials

Paraformaldehyde, melamine, TEOS, $FeCl_3 \cdot 6H_2O$, oleic acid, 1-octadecylene, CA, chloroauric acid ($HAuCl_4$), $NH_3 \cdot H_2O$ (28%), NaOH, HCl standard solution (1 mol·$L^{-1}$), sodium citrate di-hydrate, BSA, trypsin from bovine pancreas, DA, Tris , $NaBH_4$, $Na_2HPO_4$, MB and BAEE were purchased from Aladdin Chemistry Co., Ltd. (Shanghai, China). PAH (Mw 15000) was purchased from Aldrich-Sigma (St. Louis, USA). Methanol, ethanol and THF were obtained from Sinopharm Chemical Reagent Co., Ltd. (Shanghai, China). Double-distilled water (dd water) was used in the following experiment. All reagents were analytical reagents and used without further purification.

### Preparation of SPION and its aqueous phase transfer by ligand exchange

Hydrophobic SPION were synthesised with the method reported previously. The hydrophobic SPION were then transferred into water phase by ligand exchange with CA.[25]

### Preparation of silica coated MF microspheres

Uniform MF microspheres were prepared via our previous method.[23] Three different size of MF microspheres were prepared by regulating the volume ratio of prepolymer and HCl solution. Subsequently, the obtained MF microspheres were coated with silica through TEOS hydrolysation. Approximately 2g of MF microsphere was added into the mixed solution containing 400 mL of ethanol, 100 mL of dd water and 10 mL of $NH_3 \cdot H_2O$. Afterwards, 2 mL of TEOS was dropped to the solution within one hour, and the reacting mixture was stirred overnight. The final MF microspheres (MF@$SiO_2$) were collected at 5000 rpm for 5 min and washed with water at least three times.

### Preparation of magnetically adjustable magnetic microsphere fabricated by polyelectrolyte LbL assembly

The cationic polyelectrolyte PAH was utilised to assemble hydrophilic SPION on the MF@$SiO_2$ surface. About 20 mg of MF@$SiO_2$ was dispersed in 5 mL of PAH (1 mg·$mL^{-1}$ in $H_2O$), with pH adjusted to 9 with 1 mol·$L^{-1}$ of NaOH, centrifuged and washed with Tris (10 mmol·$L^{-1}$) for three times. The positively charged MF@$SiO_2$ was subsequently dispersed in 5 mL of (1 mg·$mL^{-1}$) hydrophilic SPION, with pH similarly adjusted to 9 with 1 mol·$L^{-1}$ of NaOH, followed by washing with the same Tris buffer for three times. For each kind of MF@$SiO_2$ microspheres, magnetic microspheres containing different amounts of SPION were prepared by varying the number of SPION-PAH layers. Each kind of MF@$SiO_2$ microspheres was covered with three different numbers of SPION-PAH layers (one layer, two layers and five layers). For the outer silica layer coating, about 120 mg of MF@$SiO_2$ covered with hydrophilic SPION was dispersed in the mixture of 40 mL of ethanol, 10 mL of dd water and 3 mL of $NH_3 \cdot H_2O$. Afterwards, 120 µL of TEOS was dropped into the mixture within one hour and stirred overnight. The obtained microspheres were collected at 5000 rpm for 5 min and washed with water at least three times. The MF@$SiO_2$ covered with different number of SPION-PAH layers (one layer, two layers and five layers) was signed as MS-1, MS-2 and MS-5. After drying at 60 °C, all microspheres were calcined at 600 °C for 3 h in air.

### Preparation of magnetic microsphere-immobilised trypsin

Polydopamine layer was used to immobilise protein on magnetic microspheres. For DA polymerization, approximately 30 mg of CS(2.0)-5 was ultrasonically dispersed in 30 mL of 10 mmol·$L^{-1}$ Tris prior dissolving of 0.01 mg·$mL^{-1}$ DA. The mixture was stirred for 12 h, centrifuged at 5000 rpm for 2 min and washed with dd water at least three times. The harvested CS(2.0)-5 covered with polydopamine [CS(2.0)-5@PDA] was in 30 mL of 50 mmol·$L^{-1}$ $Na_2HPO_4$ containing 100 µg·$mL^{-1}$ of BSA or trypsin. The mixture was stirred for 24 h and washed with dd water at least three times. The final amount of protein immobilised on CS(2.0)-5@PDA was quantified by Bradford method.

### Preparation of magnetic iron oxide-gold heterogeneous catalysts

Citrate-stabilised AuNPs was synthesised by the classical method. Briefly, 10 mL of 10% sodium citrate di-hydrate was added into 200 mL of dd water. When the mixture was boiling, 4 mL of 1% $HAuCl_4$ was quickly added into the boiled mixture, which was stirred for another 15 min. LbL assembly method was still used in assembling AuNPs onto microspheres. PAH was introduced to conjugate both negatively charged SPION and AuNPs. The process was expounded as follows: approximately 250 µL of MS(2.0)-5 without outer silica layer covered with PAH was dropped into 5 mL of citrate-stabilised AuNPs, separated by centrifugation at 5000 rpm for 5 min and washed with dd water at least three times. The amount of assembled AuNPs was determined by UV-vis absorptance spectra. The obtained microspheres were then coated with silica via the method above in preparation of magnetically adjustable magnetic microsphere fabricated by polyelectrolyte LbL assembly. The silica-coated microspheres containing both SPION and Au NPs were labelled as MS(2.0)-5-Au. The final microspheres signed as CS(2.0)-5-Au were obtained by calcination at 600 °C for 3 h in air of MS(2.0)-5-Au. Furthermore, hollow microspheres without SPION were also prepared by directly assembling Au NPs on cationic MF(2.0)@$SiO_2$-covered PAH, then covered with another silica layer and calcined at 600 °C for 3 h, which were named CS(2.0)-Au to compare the catalytic efficiency .

### Characterisation of microspheres: morphologies, EDX mapping, FITR spectra, TGA/DSC, UV-vis, VSM and XRD

A TEM (JEOL JEM-3010, Tokyo, Japan) with a 300 kV electron source was used to observe the morphologies of SPION, as well as the magnetic microspheres before and after calcination. Meanwhile, a SEM (Phenom G2 Pro, New York, USA) was used to scan the size distribution of magnetic microspheres before and after calcination. The hydrodynamic radius was measured by a Malvern Zetasizer (Nano ZS90, Malvern, UK). TEM images and EDX mapping images with element distribution (Si, Fe, Au and O) before and after calcination were measured by Tecnai G2 F20 Field Emission

Transmission Electron Microscopy. An FITR spectrometer (Bruker Optics Tensor 27, Ettlingen, Germany) was used to confirm their chemical structures, and an XRD (Shimadzu XRD-7000, Tokyo, Japan) was used to measure the crystalline type of samples. A VSM (Lake Shore 7410, Maryland, USA) was used to test the magnetic properties at room temperature. A thermogravimetric analyser (Mettler Toledo TGA/DSC 1, Zurich, Switzerland) was used measure their TGA and DSC from 50 °C to 800 °C with a temperature gradient of 10 °C. An UV-vis (UV-2600, Shimadzu Corporation, Kyoto, Japan) was used to survey the UV-vis absorptance spectra, and an ICP-AES (Shimadzu) was used to determine the ferrum content in the microspheres. The sedimentation state of MS-5 was recorded at 0, 30, 60, 90, 120, 150, 180, 210 min, 240 min and 270 min. Separation under external magnetic field was also recorded.

**Magnetic recovery and regeneration of immobilised Trypsin**

About 1 mmol·$L^{-1}$ of BAEE dissolved in 0.05 mmol·$L^{-1}$ Tris was selected as substrate to test trypsin activity. Absorbance at 253 nm was tested to identify trypsin activity. For magnetic retrieval test, CS(2.0)-5-immobilised trypsin was recovered under external magnetic field for another cycle, which was repeated eight times. After eight cycles, that trypsin was again calcined to remove the organic polydopamine layer-cross-linked inactive enzyme and then soaked in Tris (10 mmol·$L^{-1}$) to coat polydopamine to re-immobilise trypsin. To test the enzyme activity, the steps mentioned above were again carried out. The regenerating procedure was repeated for two more times, and the enzyme activity was tested for eight times in each regeneration.

**Catalytic reduction of MB dye and the reactivation of heterogeneous catalyst**

MB molecules can be reduced by $NaBH_4$ with the catalyst of AuNPs. The maximum absorbance wavelength ($\lambda_{max}$) of MB dye was changed during the reduction reaction to evaluate the catalytic efficiency. To test the catalytic efficiency of CS(2.0)-5-Au, the typical experiment was carried out. In details, about 25 μL of 1 mg·$mL^{-1}$ CS(2.0)-5-Au was homogeneously dispersed in 2.5 mL of 24 mg·$mL^{-1}$ MB. The UV-vis absorptance spectra in the range of 400-800 nm were measured every minute after immediately adding 1 mL of 15 mg·$mL^{-1}$ $NaBH_4$. In the recyclable experiment, the magnetic heterogeneous catalysts were recovered by external magnetic field, which was reused in another cycle after being washed with water three times. The recovering procedure was repeated for five times. To reactivate the inactive catalyst, calcination at 400 °C for 3 h was applied to reactivate damaged catalyst. The magnetic recyclable experiment was again conducted for five times. Furthermore, the reactivation by calcination and subsequent magnetic recyclable experiment was carried out for four more times. The magnetic recovery cycle experiment was also performed on MS(2.0)-5-Au when its gold content was the same as the CS(2.0)-5-Au used in the recyclable catalytic experiment above. The values of catalytic rate constant were recorded. The CS(2.0)-5 and CS(2.0)-Au catalysts were also measured to compare with CS(2.0)-5-Au using the method above.

## Conclusions

We prepared the novel thermo-stable hollow magnetic microspheres by LbL assembly on a uniform MF resin microspheres template coated by silica and calcination. Their sizes and saturation magnetizations can be regulated by different conditions. Combined with magnetic separation and calcination activation or regeneration, these microspheres with AuNPs can be reused for over 20 times for AuNPs catalyst and for trypsin catalyst reconjugation for over 32 times while maintain over 85% of average trypsin activation, hence they have more recyclable times for catalysis, lower costs and less pollute environments in application, indicating their considerable potential for recyclable catalytic applications.

## Acknowledgements

This study was supported by National Basic Research Program 973 of China (No. 2011CB707903), the National Nature Science Foundation of China (Nos. 81271686, 81228011 and 81471771).

## Notes and references

1 M. Shao, F. Ning, J. Zhao, M. Wei, D. G. Evans and X. Duan, *J. Am. Chem. Soc.*, 2012, **134**, 1071-1077.
2 C. Ma, C. Li, N. He, F. Wang, N. Ma, L. Zhang, Z. Lu, Z. Ali, Z. Xi and X. Li, *J. Biomed. Nanotechnol.*, 2012, **8**, 1000-1005.
3 Y. Wang, B. Zou, T. Gao, X. Wu, S. Lou and S. Zhou, *J. Mater. Chem.*, 2012, **22**, 9034-9040.
4 Z. Liu, H. Wang, B. Li, C. Liu, Y. Jiang, G. Yu and X. Mu, *J. Mater. Chem.*, 2012, **22**, 15085-15091.
5 S. Zhang, S. Gao and G. Gao, *Appl. Biochem. Biotechnol.*, 2010, **160**, 1386-1393.
6 L. Kong, X. Lu, X. Bian, W. Zhang and C. Wang, *ACS Appl. Mater. Interfaces*, 2010, **3**, 35-42.
7 M. Zhu and G. Diao, *J. Phys. Chem. C*, 2011, **115**, 24743-24749.
8 S. Xuan, F. Wang, J. M. Lai, K. W. Sham, Y.-X. J. Wang, S.-F. Lee, J. C. Yu, C. H. Cheng and K. C.-F. Leung, *ACS Appl. Mater. Interfaces*, 2011, **3**, 237-244.
9 A. Joshi, S. Solanki, R. Chaudhari, D. Bahadur, M. Aslam and R. Srivastava, *Acta Biomater.*, 2011, **7**, 3955-3963.
10 K. W. Bong, S. C. Chapin and P. S. Doyle, *Langmuir*, 2010, **26**, 8008-8014.
11 Z. Xu, Y. Feng, X. Liu, M. Guan, C. Zhao and H. Zhang, *Colloid Surf. B-Biointerfaces*, 2010, **81**, 503-507.
12 T. Zeng, X. Zhang, H. Niu, Y. Ma, W. Li and Y. Cai, *Appl. Catal. B-Environ.*, 2013, **134**, 26-33.
13 B. Liu, W. Zhang, F. Yang, H. Feng and X. Yang, *J. Phys. Chem. C*, 2011, **115**, 15875-15884.
14 L. Zhou, C. Gao and W. Xu, *Langmuir*, 2010, **26**, 11217-11225.
15 X. Wang, Y. Cui, Y. Wang, X. Song and J. Yu, *Inorg. Chem.*, 2013, **52**, 10708-10710.
16 W. Qin, Z. Song, C. Fan, W. Zhang, Y. Cai, Y. Zhang and X. Qian, *Anal. Chem.*, 2012, **84**, 3138-3144.
17 X. Luo and L. Zhang, *Biomacromolecules*, 2010, **11**, 2896-2903.
18 T. Yao, T. Cui, H. Wang, L. Xu, F. Cui and J. Wu, *Nanoscale*, 2014, **6**, 7666-7674.
19 Y. Zhu, J. Shen, K. Zhou, C. Chen, X. Yang and C. Li, *J. Phys. Chem. C*, 2010, **115**, 1614-1619.
20 F. Chen, R. Shi, Y. Xue, L. Chen and Q.-H. Wan, *J. Magn. Magn. Mater.*, 2010, **322**, 2439-2445.
21 Y. Li, Y. Wu, C. Luo, F. Yang, L. Qin, T. Fu, G. Wei, X. Kang and D. Wu, *J. Mat. Chem. B*, 2013, **1**, 4644-4654.



 

22 J. Park, K. An, Y. Hwang, J.-G. Park, H.-J. Noh, J.-Y. Kim, J.-H. Park, N.-M. Hwang and T. Hyeon, *Nat. Mater.*, 2004, **3**, 891-895.
23 Y. Wu, Y. Li, L. Qin, F. Yang and D. Wu, *J. Mat. Chem. B*, 2013, **1**, 204-212.
24 B. P. Pichon, P. Louet, O. Felix, M. Drillon, S. Begin-Colin and G. Decher, *Chem. Mat.*, 2011, **23**, 3668-3675.
25 Y. Liu, T. Chen, C. Wu, L. Qiu, R. Hu, J. Li, S. Cansiz, L. Zhang, C. Cui and G. Zhu, *J. Am. Chem. Soc.*, 2014, **136**, 12552-12555.
26 T. Nakamura, Y. Yamada and K. Yano, *J. Mater. Chem*, 2006, **16**, 2417-2419.
27 A. H. Lu, T. Sun, W. C. Li, Q. Sun, F. Han, D. H. Liu and Y. Guo, *Angew. Chem.-Int. Edit.*, 2011, **50**, 11765-11768.
28 R. Cui, C. Liu, J. Shen, D. Gao, J. J. Zhu and H. Y. Chen, *Adv. Funct. Mater.*, 2008, **18**, 2197-2204.
29 B. Friedel and S. Greulich-Weber, *Small*, 2006, **2**, 859-863.
30 H. Li, R. Wang, H. Hu and W. Liu, *Appl. Surf. Sci.*, 2008, **255**, 1894-1900.
31 W.-M. Zhang, X.-L. Wu, J.-S. Hu, Y.-G. Guo and L.-J. Wan, *Adv. Funct. Mater.*, 2008, **18**, 3941-3946.
32 S.-L. Shen, W. Wu, K. Guo, H. Meng and J.-F. Chen, *Colloid Surf. A-Physicochem. Eng. Asp.*, 2007, **311**, 99-105.
33 A. Mamedov, J. Ostrander, F. Aliev and N. A. Kotov, *Langmuir*, 2000, **16**, 3941-3949.
34 Y. Liu, K. Ai and L. Lu, *Chem. Rev.*, 2014, **114**, 5057-5115.
35 H. Lee, J. Rho and P. B. Messersmith, *Adv. Mater.*, 2009, **21**, 431-434.
36 E. F. Fang, J. H. Wong and T. B. Ng, *J. Biosci. Bioeng.*, 2010, **109**, 211-217.
37 S. Lin, Z. Lin, G. Yao, C. Deng, P. Yang and X. Zhang, *Rapid Commun. Mass Spectrom.*, 2007, **21**, 3910-3918.
38 Y. Li, X. Xu, C. Deng, P. Yang and X. Zhang, *J. Proteome Res.*, 2007, **6**, 3849-3855.
39 S. Lin, G. Yao, D. Qi, Y. Li, C. Deng, P. Yang and X. Zhang, *Anal. Chem.*, 2008, **80**, 3655-3665.
40 M. Demir, M. Şenel and A. Baykal, *Appl. Surf. Sci.*, 2014, **314**, 697-703.
41 C. M. Niemeyer, L. Boldt, B. Ceyhan and D. Blohm, *Anal. Biochem.*, 1999, **268**, 54-63.
42 G. Zhao, J. Wang, Y. Li, X. Chen and Y. Liu, *J. Phys. Chem. C*, 2011, **115**, 6350-6359.
43 D. Dumbre, P. Yadav, S. Bhargava and V. Choudhary, *J. Catal.*, 2013, **301**, 134-140.
44 T. Mitsudome and K. Kaneda, *Green Chem.*, 2013, **15**, 2636-2654.
45 M. Chen, P. Liu, C. Wang, W. Ren and G. Diao, *New J. Chem.*, 2014, **38**, 4566-4573.
46 Y. Xie, B. Yan, H. Xu, J. Chen, Q. Liu, Y. Deng and H. Zeng, *ACS Appl. Mater. Interfaces*, 2014, **6**, 8845-8852.
47 T. Zeng, X. Zhang, S. Wang, Y. Ma, H. Niu and Y. Cai, *J. Mat. Chem. A*, 2013, **1**, 11641-11647.
48 Q. An, M. Yu, Y. Zhang, W. Ma, J. Guo and C. Wang, *J. Phys. Chem. C*, 2012, **116**, 22432-22440.
49 H. Woo, J. W. Kim, M. Kim, S. Park and K. H. Park, *RSC Adv.*, 2015, **5**, 7554-7558.
50 X. Yan, X. Wang, Y. Tang, G. Ma, S. Zou, R. Li, X. Peng, S. Dai and J. Fan, *Chem. Mat.*, 2013, **25**, 1556-1563.
51 Z.-c. Zhang, B. Xu and X. Wang, *Chem. Soc. Rev.*, 2014, **43**, 7870-7886.
52 F.-h. Lin and R.-a. Doong, *J. Phys. Chem. C*, 2011, **115**, 6591-6598.

# Thermo-stable hollow magnetic microspheres: Preparation, characterization and recyclable catalytic applications

Jingwen Ma,‡[a] Youshen Wu,‡[a] Yun Zeng,[a] Yan Li,[a] Daocheng Wu*[a]

[a] Key Laboratory of Biomedical Information Engineering of Education Ministry, School of Life Science and Technology, Xi'an Jiaotong University, Xi'an, 710049, P. R. China.

E-mail: wudaocheng@mail.xjtu.edu.cn; Tel: +86 029 82663941

We prepared the thermo-stable hollow magnetic microspheres by layer-by-layer assembly and calcination, which can be reused many times for catalyst.